 DOI: 10.35382/TVUJS.14.8.2024.107

INTERVAL OBSERVER DESIGN FOR A WIND ENERGY CONVERSION SYSTEM

Loc Phuoc Nguyen[1*], Khai Nguyen Dang[2], Tin Trung Chau[3], Linh Nguyen[4], Ton Duc Do[5]

Abstract – *This research discusses unknown input interval observers for discrete-time wind turbine-generator systems. Firstly, the paper presents a reliable interval observer for a linear parameter-varying (LPV) system with unknown and immeasurable parameters. Secondly, systems should be considered to jointly estimate the state and unknown inputs. To address this challenge, the study develops an interval observer for a discrete-time system incorporating unknown parameter vectors. These estimating techniques rely on the insertion of extra weighting matrices to assist in reducing the impact of system uncertainties and to guarantee the stability and cooperation of the interval observers. Examples are simulated by MATLAB/Simulink software to demonstrate the effectiveness of the algorithms.*

Keywords: interval observer, linear parameter-varying (LPV), MATLAB/Simulink, system uncertainties, wind turbine.

I. INTRODUCTION

One of the most accessible and promising renewable energy sources in recent times has been wind energy. On the one hand, wind turbine installation and upkeep are rather costly. This issue becomes more significant in the case of offshore wind turbines. Similar to any other system, wind turbines can make mistakes. The control system is essential to identify, mitigate, and accommodate problems in wind turbines as it has access to data from several wind turbine components. Unplanned maintenance can be expensive for an offshore wind turbine. Consequently, it's imperative to design a control system that can autonomously detect and isolate issues as they emerge, maintain the wind turbine's overall functionality, and provide enough performance for the broken system without requiring it to be shut down.

Interval observers explain an essential method for managing systems impacted by diverse disruptions and measurement noise. They give upper and lower limits on the actual state using a dynamic structure with two outputs of Şahin [1]. Understanding the limits of starting state values and measurement noise and disruptions is necessary for this sophisticated kind of observer. Even with these constraints usually satisfied in practical settings interval estimation overcomes the drawbacks of classical observers, who can only provide asymptotic estimates without disruptions. This method is built on the theoretical basis of Kara el al. [2] and has been extended to a variety of domains, such as linear systems in studies conducted by Zhao et al. [3], Chan et al. [4], McMillan et al. [5], nonlinear systems from Peng et al. [6], fuzzy systems of Tinga [7], and applications such as fault detection, control, and monitoring of Kim et al. [8] and Calabrese et al. [9].

Real systems frequently experience noise, interruptions, and uncertain inputs. For wind turbine systems, this situation has been studied by Lei et al. [10], Heo et al. [11], Venkata et al. [12], and Liu et al. [13]. Continuous-time wind turbine systems with uncertain inputs have also been the subject of some investigations [14,

[1]Vinh Long University of Technology Education, Vietnam

[2]PhD student at Conservatoire National des arts et métiers, Paris, France

[3,5]School of Eng. and Digital Sciences (SEDS), Nazarbayev University Astana, Kazakhstan

[4]Institute of Innovation, Science and Sustainability Federation University, Australia

*Corresponding author: locnp@vlute.edu.vn

Received date: 30^{th} June 2024; Revised date: 14^{th} November 2024; Accepted date: 13^{th} January 2025

15]. However, there has not been a thorough discussion in the literature yet about the design of interval observers for discrete-time wind turbine systems with uncertain inputs. However, because switching the system from continuous to discrete time modifies stability features and necessitates correcting the estimating technique for the unknown input, the estimators suggested in this study are not directly derived.

Firstly, a novel observer structure that provides additional design degrees of freedom and loosens design requirements is developed in this work, which makes three primary contributions. Secondly, it concurrently gives interval estimates of states and unknown inputs for an uncertain discrete-time linear system. Lastly, the interval approach is used to ensure that the condition and aerodynamic torque of a wind turbine are estimated.

Below is the arrangement of the article: In Part II, the principal findings are outlined and supported. Section III concludes the work with concluding observations. Section IV then presents the simulation findings, which are presented and contrasted with the method of Wang et al. [16].

II. MAIN RESULTS

A. Studied system

The system operates discretely inside the examined wind energy conversion system of Le et al. [17].

$$\begin{cases} \omega(k+1) &= -a_d\omega(k) - b_dT_e(k) + b_dT_a(k) + f_dd(k) \\ y(k) &= c_d\omega(k) \end{cases} \quad (1)$$

Where:

$\omega(k) \in R, y(k) \in R, T_e \in R, T_a \in R, d(k) \in R$ are the state, the measured, the electromagnetic torque, the aerodynamic torque that needs to be estimated, and the unknown disturbance vectors, respectively.

The value is defined as follows: $a_d = \frac{B}{J}, b_d = \frac{1}{J}, f_d = \frac{1}{J+\Delta J}$, where J represents the mechanical inertia, B denotes the coefficient of viscous friction, and f_d corresponds to the coefficient of noise.

Both the disturbance d(k) and the starting condition of $\omega(k)$ are limited yet uncertain.

$$\underline{\omega}(k) \le \omega(k) \le \overline{\omega}(k), \quad (2)$$

$$\underline{d} \le d(k) \le \overline{d}. \quad (3)$$

where $\underline{\omega}(k), \bar{\omega}(k), d, \bar{d}$ are known vectors.

B. Preliminary transformation

From Equation (1), the study obtained an equation as Equation (4).

Equation (1) may be recast into a discrete-time LTI descriptor system as sot Equation (5) by interpreting the unknown inputs as auxiliary states.

$$\omega(k+1) - b_dT_a(k) = \quad (4)$$
$$-a_d\omega(k) - b_dT_e(k) + f_dd(k).$$

where:

$$x(k) = \begin{bmatrix} \omega(k) \\ T_a(k-1) \end{bmatrix}, E_d = \begin{bmatrix} I & -b_d \\ 0 & 0 \end{bmatrix}, A_d$$
$$= \begin{bmatrix} -a_d & 0 \\ 0 & 0 \end{bmatrix} B_d = \begin{bmatrix} -b_d \\ 0 \end{bmatrix}, F_d = \begin{bmatrix} f_d \\ 0 \end{bmatrix}, C_d = [C \quad 0].$$

Without loss of generality, it is assumed that Equation (5) is observable [18, 19].

C. Interval observer for state and disturbance

The observer is introduced as Equation (6).

$$\begin{cases} \bar{x}(k+1) = TA_d\bar{x}(k) + TB_dT_e(k) + L\big(y(k) - C_d\bar{x}(k)\big) \\ \qquad +Ny(k+1) + (TF_d)^+\bar{d} - (TF_d)^-\underline{d} \\ \underline{x}(k+1) = TA_d\underline{x}(k) + TB_dT_e(k) + L(y(k) - \underline{C}d\underline{x}(k))' \\ \qquad +Ny(k+1) + (TF_d)^+\underline{d} - (TF_d)^-\bar{d} \end{cases} \quad (6)$$

Where $T \in R^(2\times 2) and N \in R^(2\times 1)$ are the matrices to be chosen as Equation (7).

$$TE_d + NC_d = \begin{bmatrix} 1 & 0 \\ 0 & 1 \end{bmatrix}. \quad (7)$$

For example, it can be chosen for all real values t_{12} and t_{22}:

$$T = \begin{bmatrix} 0 & t_{12} \\ -\frac{1}{b_d} & t_{22} \end{bmatrix}, N = \begin{bmatrix} 1 \\ \frac{1}{b_d} \end{bmatrix}$$

Thus, we have a notation as Equation (8).

$$(TF_d)^+ = \left[\max\left\{0, -\frac{f_d}{b_d}\right\}\right], (TF_d)^- = \left[\max\left\{0, -\frac{f_d}{b_d}\right\} + \frac{f_d}{b_d}\right].$$

The following results are now ready to be stated and proved:

Theorem 1. If there exists a matrix $L \in R^{(}2 \times 1)$ such that $TA_d - LC_d \geq 0$ and $TA_d - LC_d$ Schur stable then (6) is an interval observer for the state and the aerodynamic torque of (1).

Proof. Initially, we shall rewrite Equation (5) by multiplying both sides of the equation T.

$$E_d x(k+1)T = (x(k)A_d + T_e(k)B_d + d(k)F_d)T. \quad (8)$$

Equation (8) is used to replace $E_d T = I - C_d N$ obtained

$$\begin{aligned} & x(k+1)\left(I - C_d N\right) = \left(A_d x(k) + T_e(k)B_d + d(k)F_d\right)T \\ \Leftrightarrow\ & x(k+1) = A_d x(k)T + B_d T_e(k)T + TF_d d(k) + C_d x(k+1)N \\ \Leftrightarrow\ & x(k+1) = TA_d x(k) + TB_d T_e(k) + TF_d d(k) + Ny(k+1). \end{aligned} \quad (9)$$

For each, the upper and lower error equations are taken into account.

$$\begin{cases} \bar{e}(k) = \bar{x}(k) - x(k) \\ \underline{e}(k) = x(k) - \underline{x}(k). \end{cases} \quad (10)$$

The goal is to demonstrate the non-negative and limited nature of $\bar{e}(k)$ and $\underline{e}(k)$. The following describes the upper and lower error dynamics.

$$\begin{cases} \bar{e}(k+1) = & \bar{x}(k+1) - x(k+1) \\ \underline{e}(k+1) = & x(k+1) - \underline{x}(k+1) \end{cases}. \quad (11)$$

From Equations (6) and (11) we obtain:

$$\begin{cases} \bar{e}(k+1) = & (TA_d - LC_d)\bar{e}(k) + (TF_d)^+\bar{d} - (TF_d)^-\underline{d} \\ & -TF_d d(k) \\ \underline{e}(k+1) = & (TA_d - LC_d)\underline{e}(k) - \left[(TF_d)^+\underline{d} - (TF_d)^-\bar{d}\right] \\ & +TF_d d(k). \end{cases} \quad (12)$$

And the following lemma is presented.

Lemma 1: Given a vector $x_k with x_k^- \leq x_k \leq x_k^+$ and matrix A, the inequalities hold.

$$A^+ x_k^- - A^- x_k^+ \leq Ax_k \leq A^+ x_k^+ - A^- x_k^-. \quad (13)$$

where $A^+ = max[0, A]$ and $A^- = A^+ - A$.

With the Inequality (13), we can transform it into a new inequality as follows:

$$A^+ x_k^+ - A^- x_k^- - Ax_k \geq 0. \quad (14)$$

By incorporating the above inequality with the disturbance Equation (3), we can derive that:

$$(TF_d)^+\bar{d} - (TF_d)^-\underline{d} - (TF_d)d(k) \geq 0. \quad (15)$$

Then, to have a non-negative upper bound error, the equation $TA_d - LC_d$ must be non-negative (i.e., $TA_d - LC_d \geq 0$). We can deduce the same conclusion for the lower bound error. Therefore, we need to choose L such that $TA_d - LC_d$ is non-negative and Schur stable. In the above example, when the size dimension is 2, and the form of the T and N matrices can be specified, one can choose.

$$L = \begin{bmatrix} -\frac{1}{2} \\ l_{21} \end{bmatrix}$$

such that $\frac{a_d}{b_d} - l_{21} \geq 0$. An example of the simulation will be given in the upcoming Section III.

III. SIMULATION EXAMPLE

Example 1. We will start with a continuous-time system in this instructive example, which has the system equation:

$$\frac{d\omega}{dt} = \frac{1}{Jn_{gb}}T_a - \frac{B}{J}\omega - \frac{1}{J}T_e + d. \quad (16)$$

The value and disturbance must be estimated when certain uncertainties and unknown disturbances exist (d). They have specific criteria in Table 1 that make them quantifiable.

Table 1: The system parameters

Symbol	Quantity	Value	Unit
J	Mechanical inertia	7.856	$kg.m^2$
B	Viscous friction coefficient	0.02	$kg.m^2/s$
n_{gb}	Gearbox ratio	1	-

T_e is computed using the accompanying formula:

$$T_e = \frac{3}{2}\varphi_m N_p i_q(t). \quad (17)$$

with a blade length of 10 m and an efficiency of 40%, operating at a voltage of 220 V for 1 second at a speed of 15 km/h, air pressure of 1,013.25 hPa at 15^{o}C, and φ = 0.2867 V.S/rad, Np = 14, iq = 25 A. With (n_{gb} = 1), we shall discretize the aforementioned system using the notion of derivation:

$$\frac{\omega(k+1)-\omega(k)}{\Delta t} = \frac{T_a}{J} - \frac{B}{J}\omega(k+1) - \frac{T_e}{J} + d. \quad (18)$$

Δt will have an approximate value of 0. We can also set:

$$a_d = \frac{B}{J}, b_d = \frac{1}{J}$$

and rewrite the system by multiplying the Δt:

$$\omega(k+1) = \omega(k) + \Delta t b_d T_a(k) - \Delta t a_d \omega(k) - \Delta t b_d T_e + \Delta t d(k)$$
$$\Leftrightarrow \omega(k+1) - \Delta t b_d T_a(k) = (1 - a_d \Delta t)\omega(k) - \Delta t b_d T_e + \Delta t d(k). (18)$$

We can rewrite the system in the form of equation (4) and have the following matrices:

$$A = \begin{bmatrix} 1 - a_d\Delta t & 0 \\ 0 & 0 \end{bmatrix}, B = \begin{bmatrix} -b_d\Delta t \\ 0 \end{bmatrix}, C = \begin{bmatrix} 1 & 0 \end{bmatrix}$$
$$F = \begin{bmatrix} \Delta t \\ 0 \end{bmatrix}, E_d = \begin{bmatrix} 1 & -b_d\Delta t \\ 0 & 0 \end{bmatrix}, x(k) = \begin{bmatrix} \omega(k) \\ T_a(k-1) \end{bmatrix}$$

Once the numerical value is applied, we obtain:

$$a_d = \frac{B}{J} = \frac{0.002}{7.856} = 2.546 \times 10^{-3}$$
$$b_d = \frac{1}{J} = \frac{1}{7.856} = 0.1273$$

The matrix T, N, and L has the following form:

$$T = \begin{bmatrix} 0 & t_{12} \\ -\frac{1}{b_d\Delta t} & t_{22} \end{bmatrix}, N = \begin{bmatrix} 1 \\ \frac{1}{b_d\Delta t} \end{bmatrix}, L = \begin{bmatrix} -\frac{1}{2} \\ l_{21} \end{bmatrix}$$

such that $\frac{a_d\Delta t - 1}{b_d\Delta t} - l_{21} \leq 0$. The status of the simulation findings is as follows, with the disruption shown as Figure 1.

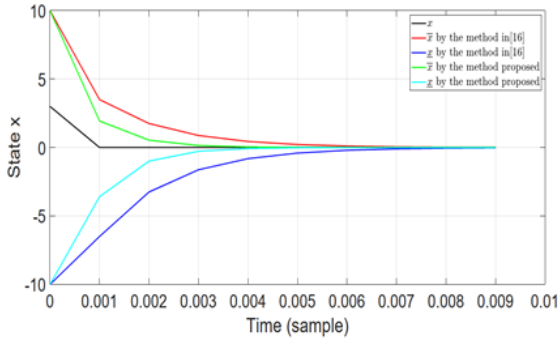

Fig. 1: Real state and Simulation of x in MATLAB

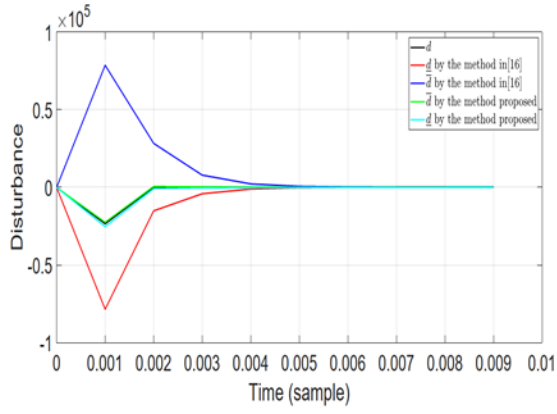

Fig. 2: Real and Simulation of disturbance in MATLAB

The estimated boundaries using the interval observer in Wang et al. [16] and the interval estimation results produced using the author's technique are displayed in Figures 1 and 2. Compared to the boundaries predicted by the interval observer in Wang et al. [16], the interval

estimates supplied by the suggested technique are more accurate representations of the real states. This result validates the suggested observer's robustness.

Example 2. We will start this part by simulating a wind turbine using the Simulink system and the LQR controller. This section presents Simulation experiments demonstrating the proposed control mechanism's effectiveness. Let's examine a WECS with table 2 specs that are based on a PMSG. The wind profile is chosen with a turbulence intensity of 10% and a mean velocity of 12.13 m/s. The construction of observer equation (6), which is provided in two figures, is inspired by the profile shown in Figure 3. Figure 4 displays the block diagram of the suggested interval observer.

Table 2: Wind energy conversion system parameters

Symbol	Parameter PMSG	Value	Unit
P_{rated}	Rated power	5	kW
P	Pole pairs	14	-
R_s	Stator resistance	0.3676	Ω
L	Stator inductance	3.55	mH
Ψ_m	Magnet flux linkage	0.2867	V·s/rad
J	Mechanical inertia	7.856	$kg \cdot m^2$
B_v	Viscous friction coefficient	0.02	$kg.m^2/s$
	Wind Turbine Parameters		
R_r	Rotor radius	1.84	m
	Other Parameters		
ρ	Air density	1.25	kg/m^3
	Control parameters		
LQR controller	Q = diag (1000, 1, 1); R = 0.1 * diag (1, 1, 1).		

Figure 5 shows that $\bar{\omega}(k) \leq \omega(k) \leq \underline{\omega}(k)$, meaning that the actual state $\omega(k)$ is consistently situated between the higher state $\bar{\omega}(k)$ and lower $\underline{\omega}(k)$. Similarly, Figure (6) demonstrates that $\underline{T_a}(k) \leq T_a(k) \leq \bar{T}_a(k)$, signifying that the disturbance $T_a(k)$ is consistently situated between the upper state $\underline{T_a}(k)$ and lower $\bar{T}_a(k)$.

The interval estimation results obtained from the proposed technique are shown in Figure (5), together with the boundaries determined using the interval observer described in the study of Wang et al. [16]. Comparing the interval estimates from the suggested technique with the

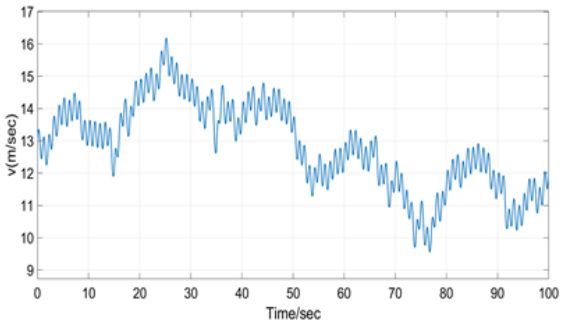

Fig. 3: Profile of wind speed with a mean speed of 12.13 meters per second from Suleimenov et al. [21]

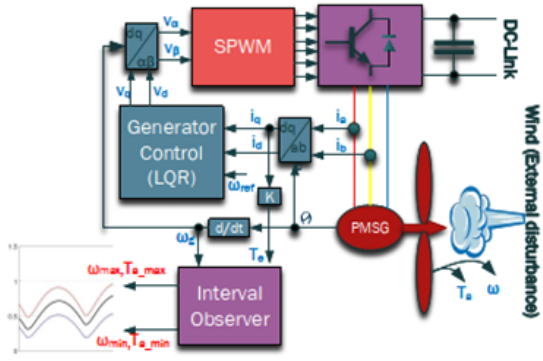

Fig. 4: Machine-side portion of WECS's back-to-back power converters

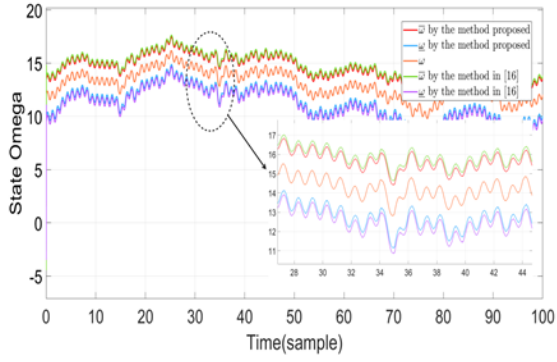

Fig. 5: The state ω and interval estimated bounds $\bar{\omega}$, $\underline{\omega}$

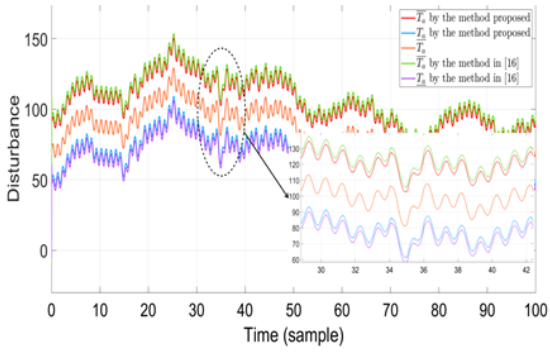

Fig. 6: The unknown input T_a and interval estimations $\bar{T}_a$, $\underline{T_a}$

boundaries calculated by the interval observer in Wang et al. [16], the technique is closer to the real states and more accurate. This proves that the suggested observer is resilient.

The simulation results indicate that this interval observer architecture works well when the upper and lower bounds constrain the primary states. This research allows for interval estimation of the disturbance and the system state, both of which have an effect on the system as a whole.

IV. CONCLUSION

This research investigates a state interval observer and simultaneous input for uncertain wind turbine switching systems. It employs a novel strategy based on the (T-N-L) technique to handle the effects of unknown disturbances and measurement noise, enabling the simultaneous estimate of the state vector and the unknown input. An interval observer with new, more flexible matrices is part of the design. The method's efficiency is demonstrated by the simulation results. Subsequent research endeavors may further refine the norm-based design methodology and expand its use to Linear-Parameter Varying switching systems.

ACKNOWLEDGMENT

The Authors thank Prof. Thach Ngoc Dinh at Conservatoire National des arts et métiers Paris, France, for his constructive remarks that improved this paper.

REFERENCES

[1] Şahin AD. Progress and recent trends in wind energy. *Progress in Energy and Combustion Science*. 2004;30(5): 501–543. https://doi.org/10.1016/j.pecs.2004.04.001.

[2] Kara T, Şahin AD. Implications of climate change on wind energy potential. *Sustainability*. 2023;15(20): 14822. https://doi.org/10.3390/su152014822.

[3] Zhao R, Shen Y. Fault detection of WECSs with a delayed input and an unknown part based on SVO. *IEEE Access*. 2020;8: 121050–121058. https://doi.org/10.1109/ACCESS.2020.3006894.

[4] Chan D, Mo J. Life cycle reliability and maintenance analyses of wind turbines. *Energy Procedia*. 2017;110: 328–333. https://doi.org/10.1016/j.egypro.2017.03.148.

[5] McMillan D, Ault GW. Quantification of condition monitoring benefit for offshore wind turbines. *Wind Engineering*. 2007;31(4): 267–285. https://doi.org/10.1260/030952407783123060.

[6] Peng H, Li S, Shangguan L, Fan Y, Zhang H. Analysis of wind turbine equipment failure and intelligent operation and maintenance research. *Sustainability*. 2023;15(10): 8333. https://doi.org/10.3390/su15108333.

[7] Tinga T, Loendersloot R. Physical model-based prognostics and health monitoring to enable predictive maintenance. In: *Predictive maintenance in dynamic systems: advanced methods, decision support tools and real-world applications*. Springer; 2019. p.313–353. https://doi.org/10.1007/978-3-030-05645-2_11.

[8] Kim W, Katipamula S. A review of fault detection and diagnostics methods for building systems. *Science and Technology for the Built Environment*. 2018;24(1): 3–21. https://doi.org/10.1080/23744731.2017.1318008.

[9] Calabrese F, Regattieri A, Bortolini M, Galizia FG. Data-driven fault detection and diagnosis: Challenges and opportunities in real-world scenarios. *Applied Sciences (Basel)*. 2022;12(18): 9212. https://doi.org/10.3390/app12189212.

[10] Lei Y, Yang B, Jiang X, Jia F, Li N, Nandi AK. Applications of machine learning to machine fault diagnosis: A review and roadmap. *Mechanical Systems and Signal Processing*. 2020;138: 106587. https://doi.org/10.1016/j.ymssp.2019.106587.

[11] Heo S, Lee JH. Fault detection and classification using artificial neural networks. *IFAC-PapersOnLine*. 2018;51(11): 470–475. https://doi.org/10.1016/j.ifacol.2018.08.380.

[12] Venkata P, Pandya V, Vala K, Sant AV. Support vector machine for fast fault detection and classification in modern power systems using quarter cycle data. *Energy Reports*. 2022;8: 92–98. https://doi.org/10.1016/j.egyr.2022.10.279.

[13] Liu R, Yang B, Zio E, Chen X. Artificial intelligence for fault diagnosis of rotating machinery: A review. *Mechanical Systems and Signal Processing*. 2018;108: 33–47. https://doi.org/10.1016/j.ymssp.2018.02.016.

[14] Mattera CG, Quevedo J, Escobet T, Shaker HR, Jradi M. A method for fault detection and diagnostics in ventilation units using virtual sensors. *Sensors (Basel)*. 2018;18(11): 3931. https://doi.org/10.3390/s18113931.

[15] Habibi H, Howard I, Simani S. Reliability improvement of wind turbine power generation using model-based fault detection and fault tolerant control: A review. *Renewable Energy*. 2019;135: 877–896. https://doi.org/10.1016/j.renene.2018.12.066.

[16] Wang Z, Lim CC, Shen Y. Interval observer design for uncertain discrete-time linear systems. *Systems & Control Letters*. 2018;116: 41–46. https://doi.org/10.1016/j.sysconle.2018.04.003.

[17] Le AV, Do TD. High-order observers-based LQ control scheme for wind speed and uncertainties estimation in WECSs. *Optimal Control Applications and Methods*. 2018;39: 1818–1832. https://doi.org/10.1002/oca.2444.

[18] Efimov D, Perruquetti W, Raïssi T, Zolghadri A. On interval observer design for time-invariant discrete-time systems. In: *Proceedings of the 2013 European Control Conference (ECC)*. 17th – 19th July 2013; Zurich, Switzerland. IEEE; 2013. p.2651–2656. https://doi.org/10.23919/ECC.2013.6669108.

[19] Efimov D, Fridman L, Raissi T, Zolghadri A, Seydou R. Interval estimation for LPV systems applying high order sliding mode techniques. *Automatica*. 2012;48(10): 2365–2371. https://doi.org/10.1016/j.automatica.2012.06.073.

[20] Zholtayev D, Rubagotti M, Do TD. Adaptive super-twisting sliding mode control for maximum power point tracking of PMSG-based wind energy conversion systems. *Renewable Energy*. 2022;183: 877–889. https://doi.org/10.1016/j.renene.2021.11.055.

[21] Suleimenov K, Sarsembayev B, Phuc BDH, Do TD. Disturbance observer-based integral sliding mode control for wind energy conversion systems. *Wind Energy*. 2020;23: 1026–1047. https://doi.org/10.1002/we.2471.